Available online at www.sciencedirect.com
ScienceDirect
Applied Catalysis B: Environmental 82 (2008) 151–156
APPLIED CATALYSIS B: ENVIRONMENTAL
www.elsevier.com/locate/apcatb

An efficient electron transfer at the Fe^0/iron oxide interface for the photoassisted degradation of pollutants with H_2O_2

Yulun Nie, Chun Hu *, Lei Zhou, Jiuhui Qu

State Key Laboratory of Environmental Aquatic Chemistry, Research Center for Eco-Environmental Sciences, Chinese Academy of Sciences, Beijing 100085, China

Received 10 July 2007; received in revised form 10 January 2008; accepted 26 January 2008
Available online 5 February 2008

Abstract

Fe-200 was synthesized through the calcination of iron powder at 200 °C for 30 min in air. On the basis of characterization by X-ray diffraction and X-ray photoelectron spectroscopy, Fe-200 had a core–shell structure, in which the surface layer was mainly composed of Fe_2O_3 with some FeOOH and FeO, and the core retained metallic iron. The kinetics and mechanism of the interfacial electron transfer on Fe-200 were investigated in detail for the photoassisted degradation of organic pollutants with H_2O_2. Under deoxygenated conditions in the dark, the generation of hydroxyl radicals in aqueous Fe-200 dispersion verified that galvanic cells existed at the interface of Fe^0/iron oxide, indicating the electron transfer from Fe^0 to Fe^{3+}. Furthermore, the effects of hydrogen peroxide and different organic pollutants on the interfacial electron transfer were examined by the change rate of the Fe^{3+} concentration in the solution. The results indicated that hydrogen peroxide provided a driving force in the electron transfer from Fe^{2+} to Fe^{3+}, while the degradation of organic pollutants increased the electron transfer at the interface of Fe^0/iron oxide due to their reaction with $^{\bullet}OH$.

Keywords: Electron transfer; Galvanic cell-like performance; Iron oxides; Iron metal

1. Introduction

Among the advanced oxidation processes (AOPs) to degrade aqueous recalcitrant organic pollutants, the Fenton reaction has attracted great attention due to its formation of highly potent chemical species, $^{\bullet}OH$, for non-selective oxidation [1,2]. However, the application of the homogeneous Fenton reaction is limited by the narrow working pH range (<4), separation and recovery of the iron species [3]. To overcome these drawbacks and extend the working pH range, some efforts have been made to develop different heterogeneous Fenton catalysts [4,5]. However, most of them showed low efficiency for practical treatment of organic pollutants at neutral pH.

Since iron is relatively inexpensive and nontoxic, it has been widely used in different environmental treatment processes. For example, utilization of Fe^0 as a chemical reductant to remove pollutants in water has been intensively investigated [6,7]. Additionally, Fe^0 has been studied as a precursor of Fe^{2+} in Fenton reactions in acid media [8,9]. However, the direct electron transfer from Fe^0 to H_2O_2 during a Fenton reaction is a very slow process at neutral pH [10]. However, recently, it has been found that a composite, enclosed zerovalent iron with iron oxide had higher reactivity in the oxidation of pollutants than zerovalent iron or mixed iron oxides alone. Fe^0/Fe_3O_4 composite prepared by mechanical alloying of Fe^0 and Fe_3O_4 powders showed highly catalytic activity for the Fenton process [10,11]. Fe–Fe_2O_3 core–shell nanowire could more efficiently degrade organic pollutants than traditional Fenton reagent Fe^{2+} ions at neutral pH when it was used in electrochemical-assisted and ultrasound-assisted Fenton-like reaction systems [1]. An in-depth understanding of the mechanism is essential to devise a strategy and apply this kind of composite in a practical system to efficiently degrade organic pollutants in water. However, only a few studies [10,11] have been conducted so far for the properties of the interface of Fe^0/iron oxides. Moreover, there is no direct evidence to indicate the mechanism of the enhanced catalytic activity of the composite by electron transfer from Fe^0 to iron oxides at the

* Corresponding author. Tel.: +86 10 62849628; fax: +86 10 62923541.
E-mail address: huchun@rcees.ac.cn (C. Hu).

0926-3373/$ – see front matter © 2008 Elsevier B.V. All rights reserved.
doi:10.1016/j.apcatb.2008.01.019

interface. The mechanism of the electron transfer from Fe^0 to iron oxide was conjectured to occur by a thermodynamically favorable process.

Recently, we have prepared enclosed Fe^0 by the mixture of Fe_2O_3 and FeOOH, which was found to be highly effective for the degradation of azodyes at neutral pH and exhibited excellent long-term stability in the presence of H_2O_2 and UVA [12]. In the present study, the catalytic mechanism of the composite was investigated in detail. For the first time, the galvanic cell-like performance of Fe^0/iron oxide was verified by the generation of hydroxyl radicals under deoxygenated conditions in the dark according to the mechanism of the oxidative electrochemical processes. Furthermore, the influences of hydrogen peroxide and different organic pollutants on the electron transfer process were also investigated in detail. These results verified that highly effective interfacial electron transfer was responsible for the high activity of Fe^0/iron oxide.

2. Experimental

2.1. Materials and reagents

Iron powder (>98.0%), dimethyl phthalate (DMP) and 2,4-dichlorophenoxyacetic acid (2,4-D) were purchased from the Yili Company. Hydrogen peroxide (30%, w/w) was purchased from the Shentai Company. All other chemicals were analytical grade. Deionized and doubly distilled water was used throughout this study. The solution pH was adjusted by diluted aqueous solution of NaOH and H_2SO_4.

The catalyst was synthesized by calcination of iron powder at 200 °C in air for different time, and the sample calcined for 30 min (Fe-200) exhibited the highest activity. This catalyst was used for all the experiments unless otherwise specified. The particle size of Fe-200 was in the range of 80–100 μm according to scanning electron microscope.

2.2. Characterization of catalysts

The X-ray powder diffraction (XRD) patterns of the catalysts were recorded on a Scintag-XDS-2000 diffractometer with Cu Kα radiation (λ = 1.54059 Å). The X-ray photoelectron spectroscopy (XPS) data were taken on an AXIS-Ultra instrument from Kratos using monochromatic Al Kα radiation (225 W, 15 mA, 15 kV) and low-energy electron flooding for charge compensation. To compensate for surface charge effects, the binding energies were calibrated using the C 1s hydrocarbon peak at 284.80 eV.

2.3. Procedures and analyses

The light source was a 300 W high-pressure mercury lamp fixed inside a cylindrical Pyrex flask, which was surrounded by a circulating water jacket to cool the lamp. The exterior of the cylindrical Pyrex flask was wrapped by tinfoil, leaving just a small window (3.5 cm × 1.5 cm) at the side face. The light was then focused onto a 100 mL glass reaction vessel. The average light intensity was 15.4 mW/cm^2. To effectively suspend the catalyst, compressed air was bubbled from the bottom of the reactor. The reaction temperature was maintained at 25 °C.

In a typical experiment, 0.1 g of catalyst were dispersed in 50 mL DMP solution (20 mg/L, pH 6.7). After the addition of H_2O_2 (10 mM) and UVA irradiation, at given time intervals, 0.5 mL samples were withdrawn and filtered through a Millipore filter (pore size 0.45 μm). The filtrates were analyzed using a high performance liquid chromatograph (HPLC, Alliance 2695) with an Xterra MS C18 column. Fifty percent acetonitrite with 50% water mobile phase was used. Determination of hydroxyl radicals was performed with a photometric method [13,14]. Fe^{2+} and Fe^{3+} concentrations were measured by a 1,10-phenanthroline method [15] with a detection limit of 1.8×10^{-7} mol/L for Fe^{2+}.

3. Results and discussion

3.1. Characterization of catalysts

Fig. 1 shows the X-ray diffraction patterns of Fe^0 and Fe-200. The two samples showed similar peaks of XRD patterns, indexed to a cubic phase with Fe^0 (JCPDS No. 06-0696). The results verified that Fe-200 still contained Fe^0 component. Fe-200 was characterized by XPS analysis. As shown in Fig. 2a, the binding energies of about 711, 719 and 725 eV were assigned to the $2p_{3/2}$, shake-up satellite $2p_{3/2}$, and $2p_{1/2}$ of Fe^{3+} ions in Fe_2O_3 or FeOOH, respectively [16]. The appearance of a weak shoulder at 709.5 eV, characteristic of the $2p_{3/2}$ of Fe^{2+} ions, suggested the presence of FeO phase [17,18]. No signal was detected for Fe^0 at 707 eV. These features indicated that the Fe-200 surface was enclosed with a layer of iron oxide. Since both Fe_2O_3 and FeOOH had similar features and peak positions in this region, O 1s survey scan was further conducted to delineate the surface oxygen states. As shown in Fig. 2b, the O 1s region can be decomposed into three peaks at 529.6, 530.9, and 531.9 eV, corresponding to O^{2-}, OH, and chemically or physically adsorbed water [16], respectively (O^{2-}:OH:H_2O = 71.24:16.39:9.24). The surface OH group

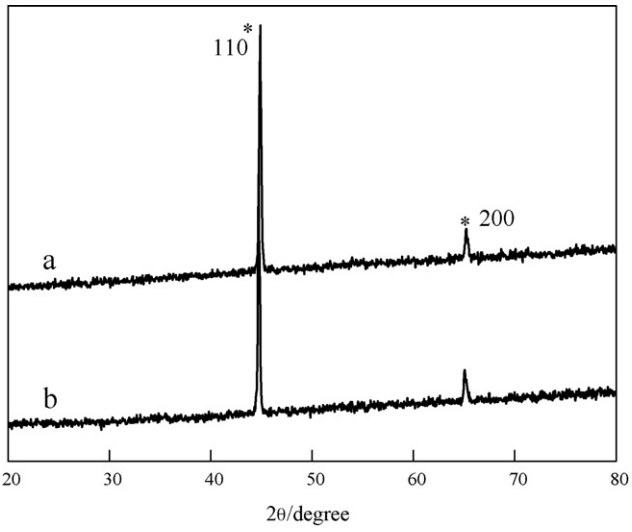

Fig. 1. XRD patterns of (a) Fe^0 and (b) Fe-200.

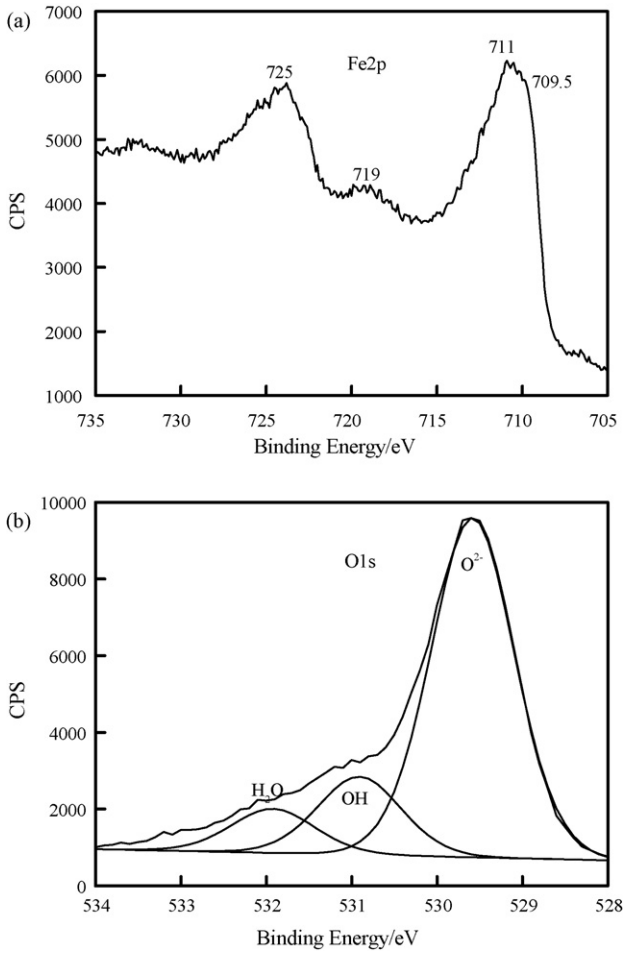

Fig. 2. XPS spectrum of Fe-200: (a) Fe2p and (b) O 1s.

suggested the existence of FeOOH on the surface of Fe-200. Furthermore, the experimental value of the ratio of Fe^{3+} to OH was 5.1, which was more than 1 (the stoichiometric ratio in FeOOH), revealing the existence of Fe_2O_3. Fe-200 thus had a core–shell structure: the outer layer was primarily comprised of Fe_2O_3 with some FeOOH and FeO present, while the core retained metallic iron.

3.2. Galvanic cell-like performance of Fe-200

Fig. 3 displays the temporal concentration changes of DMP using different iron species in the presence of H_2O_2 and UVA. Only 15% of DMP was degraded (curve a) with no catalyst. No significant degradation of DMP was observed over α-FeOOH and γ-Fe_2O_3 (curves b and c). Fe^0 exhibited some activity; about 40% of DMP was degraded (curve d). While complete abatement of DMP was obtained within 60 min in the presence of Fe-200 (curve f), only 65% degradation of DMP was obtained in the Fe^{3+}/H_2O_2/UVA system (curve e), even when the Fe^{3+} concentration in the solution was 3 mg/L, which was two times greater than the highest Fe^{3+} concentration (1.53 mg/L) detected during the reaction over Fe-200. Therefore, the introduction of iron oxide greatly enhanced the reactivity of Fe^0. Based on the redox potentials (reactions (1)–(3)), an

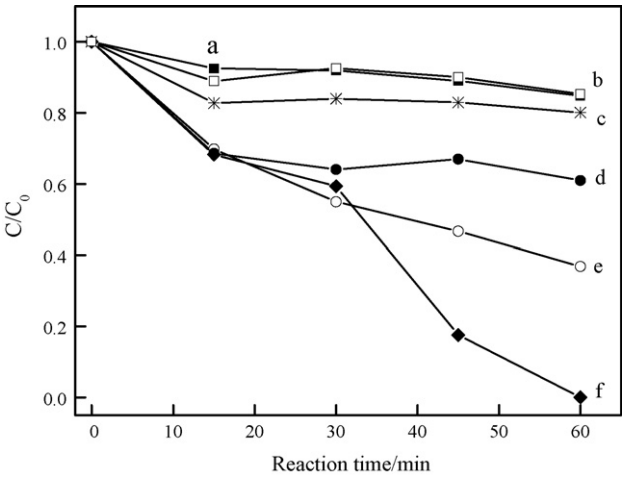

Fig. 3. Photoassisted degradation of DMP (50 mL, 20 mg/L, pH 6.5) over different catalysts in the presence of H_2O_2 (10 mM) and UVA: (a) with no catalyst, (b) α-FeOOH, (c) γ-Fe_2O_3, (d) Fe^0, (e) Fe^{3+} (3 mg/L) and (f) Fe-200. Addition of catalyst: 2 g/L.

electron transfer process is thermodynamically favorable at the interface of Fe^0/iron oxide. Thus, Fe^0/Fe^{2+} (Fe^0) serves as the cathode, and Fe^{2+}/Fe^{3+} (iron oxides) serves as the anode. Fe-200 would have galvanic cell-like performance.

$$Fe^{2+} + 2e^- \rightarrow Fe^0, \qquad E^0 = -0.440\,V \tag{1}$$

$$Fe^{3+} + 1e^- \rightarrow Fe^{2+}, \qquad E^0 = 0.771\,V \tag{2}$$

$$Fe^0 + 2Fe^{3+} \rightarrow 3Fe^{2+}, \qquad E^0 = 1.210\,V \tag{3}$$

Since under aerobic conditions, the •OH could be formed by the oxidation of Fe^0. To confirm this conjecture, under deoxygenated conditions in the dark, the generation of •OH was determined in aqueous Fe^0 and Fe-200 dispersions. As shown in Fig. 4, no significant •OH formation was observed in aqueous Fe^0 dispersion (curve a), while the quantities of •OH increased with the reaction time (curve b) in aqueous Fe-200 suspension under otherwise identical conditions. According to

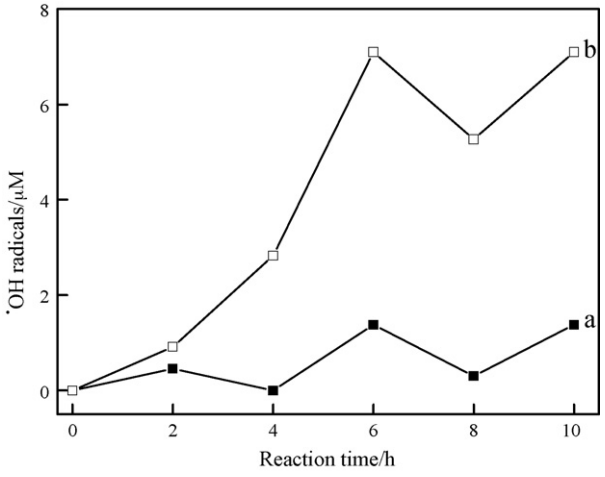

Fig. 4. Generation of hydroxyl radicals in (a) Fe^0 and (b) Fe-200 dispersions (2 g/L) at pH 7.00 as a function of reaction time under deoxygenated conditions in the dark.

the published works, in the oxidative electrochemical processes, the initial step is the discharge of water molecules to form adsorbed •OH at the anode surface whether O_2 exists or not [19–21]. Higher oxidation states on the surface of electrodes are present above the thermodynamic potential from H_2O to •OH, which is lower than 1.23 V from H_2O to oxygen [22]. Therefore, the electron potential of the interface of Fe^0/iron oxide, 1.21 V, is higher than the one from H_2O to •OH, causing •OH radicals to be produced on the surface of Fe-200 in the dark under deoxygenated conditions. This result provides a solid indication that the galvanic cell exists at the interface of Fe^0/iron oxide.

3.3. Characterization of the electron transfer process at the interface Fe^0/iron oxide

The above results confirmed that the electron transfer proceeded according to the sequence shown in reactions (1)–(3). Thus, Fe^{2+} should be the stable status. However, in the environment of oxidation, the change rate of the free Fe^{3+} concentration could indicate the electron transfer rate at the interface of Fe^0/iron oxide. To confirm this hypothesis, the changes of iron ions concentration in the solution were investigated in Fe-200 and Fe^0 dispersions in the presence of H_2O_2 and UVA at neutral pH. As shown in Fig. 5, no significant Fe^{2+} was detected for both cases. The concentration of Fe^{3+} increased rapidly with the irradiation time and reached a maximum value of 1.53 mg/L at 60 min, then decreased in Fe-200 dispersion (curve a). Meanwhile, the concentration of •OH rapidly increased and reached to the maximum at 15 min, then decreased due to the further oxidation of hydroxylation intermediates (curve b). While the concentration of Fe^{3+} was hardly changed with reaction time in Fe^0 dispersion (curve c). Similarly, the formation rate of •OH was also slower (curve d). These results indicated that the electron transfer process at the interface of Fe^0/iron oxide could be characterized by the change of Fe^{3+} concentration in the solution.

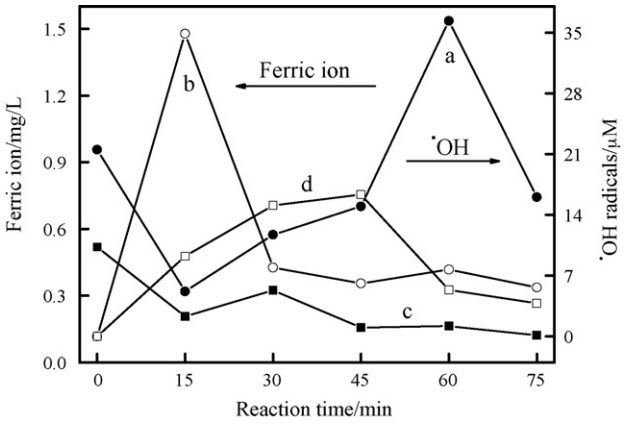

Fig. 5. Changes of ferric ion concentration and the generation of •OH during the photoassisted degradation of DMP with H_2O_2 (10 mM) over different catalysts: (a) Fe^{3+} and (b) •OH in Fe-200 dispersion, (c) Fe^{3+} and (d) •OH in Fe^0 dispersion (catalyst: 2 g/L, DMP: 20 mg/L, pH 6.5).

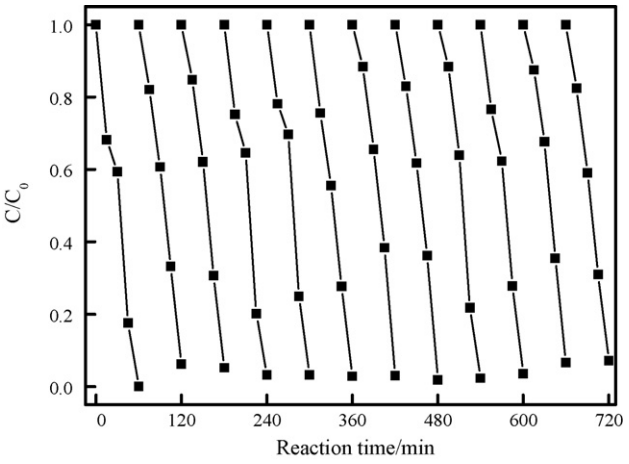

Fig. 6. Changes in the concentration of DMP (50 mL, 20 mg/L, pH 6.5) during the multicycle degradation process over Fe-200 (2 g/L) in the presence of H_2O_2 (10 mM) and UVA.

3.4. Role of H_2O_2 in enhancing the electron transfer at the interface of Fe^0/iron oxide

In the presence of H_2O_2 under UVA irradiation, Fe-200 did not exhibit any obvious loss of activity in the degradation of DMP when it was further reused for 12 cycles (Fig. 6). Oppositely, without the addition of H_2O_2, only in the first run, Fe-200 showed some activity for the degradation of DMP under UVA irradiation. In the second run, the catalyst was nearly inactive. The results indicated that hydrogen peroxide played a key role in the reuse of the catalyst. Furthermore, the concentrations of Fe^{3+} and •OH in the solution were determined in aqueous Fe-200 dispersion under UVA irradiation without H_2O_2 during the two runs (Fig. 7). In the first run, the concentration of Fe^{3+} decreased and then increased, and then decreased with reaction time, while the concentration of •OH increased with the concentration change of Fe^{3+}. The concentration of Fe^{3+} changed more slowly in the second run than that in the first run. Accordingly, no significant •OH was formed under the same conditions. Based on the results of Figs. 5 and 7, the concentration change of Fe^{3+} in the solution indicated the electron transfer at the interface of Fe-200 and the formation of •OH. The faster the concentration of Fe^{3+} changed, the more •OH radicals were formed. The results revealed that H_2O_2 provided a driving force in the recycling of Fe^{2+} to Fe^{3+}.

3.5. Effect of organic pollutants on the electron transfer at the interface of Fe^0/iron oxide

The concentration of Fe^{3+} in the solution was also determined during the degradation of different initial concentration of DMP in the Fe-200/H_2O_2/UVA system. As shown in Fig. 8, the concentration of Fe^{3+} hardly changed with reaction time (curve a) without DMP, whereas it greatly changed with reaction time in the presence of DMP, and the change frequency at 20 mg/L DMP was faster than that one of 40 mg/L (curves b and c). Correspondingly, the degradation

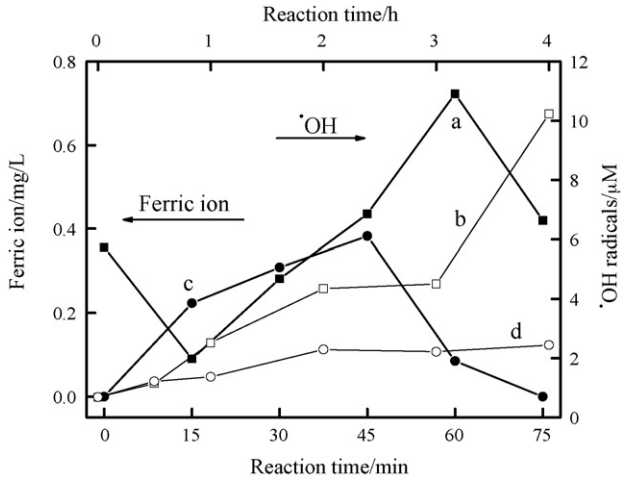

Fig. 7. Changes of ferric ion concentration and the generation of •OH with irradiation time in the recycling run of Fe-200 without of H_2O_2 for the degradation of DMP (catalyst: 2 g/L, DMP: 20 mg/L, pH 6.5): (a) Fe^{3+} and (b) •OH in first run, (c) Fe^{3+} and (d) •OH in second run.

rate of 20 mg/L DMP was also faster than that one of 40 mg/L. This result verified that the degradation of DMP consumed •OH, leading to the increase of the electron transfer. Furthermore, the concentration change of Fe^{3+} with reaction time during the degradation of DMP and 2,4-D at the same molar concentration was determined. As shown in Fig. 9, the concentration of Fe^{3+} in the solution changed more rapidly with reaction time in the degradation of 2,4-D than in the degradation of DMP at the same molar concentration. Since 2,4-D and DMP have the reaction rate constant 5×10^9 and $4 \times 10^9\ M^{-1}\ s^{-1}$ with •OH [23]. 2,4-D reacted more easily with •OH than DMP. Fig. 9 showed that 2,4-D was completely disappeared within 20 min, while only about 40% DMP was degraded. The •OH could be consumed more in the degradation of 2,4-D than that one in the degradation of DMP under the otherwise identical conditions. This result further confirmed that the degradation of organic pollutants enhanced the electron transfer process at the interface.

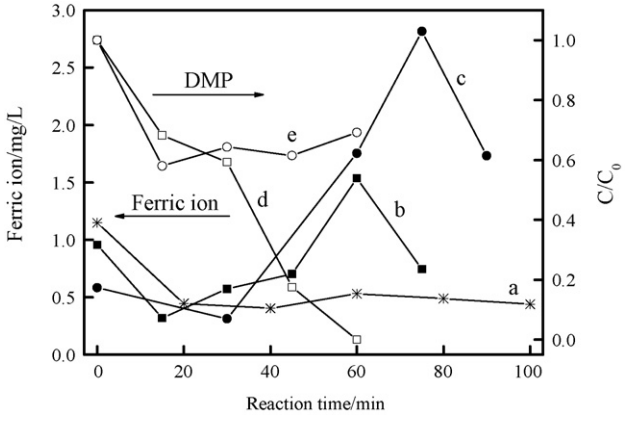

Fig. 8. Changes of Fe^{3+}, DMP concentration with reaction time in the Fe-200 (2 g/L)/H_2O_2 (10 mM)/UVA system at different initial DMP concentrations (50 mL, pH 6.5): (a) Fe^{3+} in the solution without DMP, (b) Fe^{3+} in the 20 mg/L DMP solution, (c) Fe^{3+} in the 40 mg/L DMP solution, (d) DMP 20 mg/L and (e) DMP 40 mg/L.

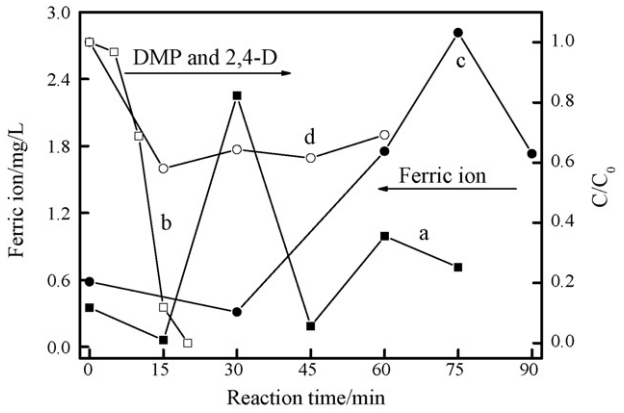

Fig. 9. Changes of Fe^{3+} concentration in the Fe-200 (2 g/L)/H_2O_2 (10 mM)/UVA system during the degradation of different organic pollutants (0.2 mM, 50 mL, pH 6.5): (a) Fe^{3+} in 2,4-D solution, (b) 2,4-D, (c) Fe^{3+} in DMP solution and (d) DMP.

4. Conclusions

The core–shell structure of Fe-200 produced a highly efficient heterogeneous photo-Fenton catalyst for the degradation of organic pollutants. The galvanic cell-like performance of Fe-200 and the interfacial electron transfer process were verified by the formation of •OH in aqueous Fe-200 suspension under deoxygenated conditions in the dark. The process of electron transfer on the surface of Fe-200 was illustrated by the change rate of the Fe^{3+} concentration in the solution. Hydrogen peroxide provided a driving force in the conversion of Fe^{2+} to Fe^{3+}. The degradation of organic pollutants increased the electron transfer at the interface of Fe^0/iron oxide due to their reaction with •OH.

Acknowledgements

This work was supported by the National Natural Science Foundation of China (No. 50778169, 50621804) and the National 863 Project of China (Grant No. 2006AA06Z304).

References

[1] Z. Ai, L. Lu, J. Li, J. Qiu, M. Wu, J. Phys. Chem. C 111 (2007) 4087.
[2] H. Liu, C. Wang, X. Li, X. Xuan, C. Jiang, H. Cui, Environ. Sci. Technol. 41 (2007) 2937.
[3] X. Lv, Y. Xu, K. Lv, G. Zhang, J. Photochem. Photobiol. A: Chem. 173 (2005) 121.
[4] J. He, W. Ma, J. He, J. Zhao, J. Yu, Appl. Catal. B: Environ. 39 (2002) 211.
[5] H. Lim, J. Lee, S. Jin, J. Kim, J. Yoon, T. Hyeon, Chem. Commun. 4 (2006) 463.
[6] L.J. Matheson, P.G. Tratnyek, Environ. Sci. Technol. 28 (1994) 2045.
[7] S.R. Kanel, J.M. Greneche, H. Choi, Environ. Sci. Technol. 40 (2006) 2045.
[8] H. Liu, X. Li, Y. Leng, C. Wang, Water Res. 41 (2007) 1161.
[9] H. Kusic, N. Koprivanac, L. Srsan, J. Photochem. Photobiol. A: Chem. 181 (2006) 195.
[10] F.C.C. Moura, M.H. Araujo, R.C.C. Costa, Chemosphere 60 (2005) 1118.
[11] F.C.C. Moura, G.C. Oliveira, M.H. Araujo, R.M. Lago, Appl. Catal. A: Gen. 307 (2006) 195.
[12] Y. Nie, C. Hu, J. Qu, L. Zhou, X. Hu, Environ. Sci. Technol. 41 (2007) 4715.
[13] M.G. Steiner, C.F. Babbs, Arch. Biochem. Biophys. 278 (1990) 478.

[14] C.F. Babbs, M.J. Gale, Anal. Biochem. 163 (1987) 67.
[15] Y. Huang, J. Li, W. Ma, M. Cheng, J. Zhao, J. Phys. Chem. B 108 (2004) 7263.
[16] X. Li, W. Zhang, Langmuir 22 (2006) 4638.
[17] A.P. Grosvenor, B.A. Kobe, M.C. Biesinger, N.S. Mclntyre, Surf. Interface Anal. 36 (2004) 1564.
[18] D.L. Ma, T. Veres, L. Clime, F. Normandin, J.W. Guan, D. Kingston, B. Simard, J. Phys. Chem. C 111 (2007) 1999.
[19] O. Simond, V. Schaller, Ch. Comninellis, J. Electrochem. Soc. 42 (1997) 2009.
[20] B. Marselli, J. Garcia-Gomez, P.A. Michaud, M.A. Rodrigo, Ch. Comninellis, J. Electrochem. Soc. 150 (2003) D79.
[21] S.E. Treimer, J. Feng, M.D. Scholten, D.C. Johnson, A.J. Davenport, J. Electrochem. Soc. 148 (2001) E459.
[22] R.S. Juang, S.W. Wang, Water Res. 34 (2000) 3179.
[23] W.R. Haag, C.C.D. Yao, Environ. Sci. Technol. 26 (1992) 1005.